

Short Communication

Three Separated Growth Sequences of Vertically-Aligned Carbon Nanotubes on Porous Silicon: Field Emission Applications

Jalal Rouhi¹, Hesamedin Khosravani Malayeri², Saeid Kakooei^{3,*}, Rouhollah Karimzadeh¹, Salman Alrokayan⁴, Haseeb Khan⁴, Mohamad Rusop Mahmood⁵

¹ Department of Physics, Shahid Beheshti University, Evin, Tehran 19839, Iran

² Department of Mechanical Engineering, Arak Branch, Islamic Azad University, Arak, Iran

³ Centre for Corrosion Research, Department of Mechanical Engineering, Universiti Teknologi PETRONAS, Tronoh31750, Malaysia

⁴ Research Chair for Biomedical Applications of Nanomaterials, Biochemistry Department, College of Science, King Saud University (KSU), Riyadh, Saudi Arabia

⁵ Centre of Nanoscience and Nanotechnology (NANO-SciTech Centre), Institute of Science, Universiti Teknologi MARA, Shah Alam, Selangor 40450, Malaysia

*E-mail: saeid.kakooei@utp.edu.my

Received: 4 May 2018 / Accepted: 25 June 2018 / Published: 1 September 2018

Three separated growth sequences of vertically-aligned carbon nanotubes (CNTs) were successfully synthesized for the first time on porous silicon (PSi) by modifying the catalyst-nanotemplate interaction in a two-stage hot filament assisted chemical vapor deposition. The morphological differences between the aligned CNTs grown by various flow rates were investigated by means of FESEM images. The presence of single-wall CNTs (SWCNTs) was confirmed by Raman radial breathing mode peak between 100 and 400 cm^{-1} . The low operating electrical field of the multilayer VACNTs grown on PSi is attributable to a relatively high field enhancement factor, which is the result of the geometrical configuration of the CNTs and the substrate. The findings demonstrate that multilayer CNTs have been identified as promising candidates for field emitters in numerous applications such as electron microscopy, flat panel display, as well as other advanced technologies.

Keywords: Multilayer structure; Carbon nanotubes; Two-stage hot filament assisted CVD; Field emission properties; Electrical properties

1. INTRODUCTION

Carbon nanotubes (CNTs) have been proposed as a novel material for a wide variety of

technological applications exploiting its unique mechanical and electrical properties, such as electron field emitters in panel displays, scanning probe microscope tips, supercapacitor electrodes, hybrid fuel cell and energy absorbing materials [1]. Among these applications, CNTs are extraordinary materials for field emission (FE), generally because of their high electrical conductivity at room temperature, high aspect ratio and whisker-like shape [2]. Many methods have been developed to synthesize high-quality CNTs, including arc discharge, laser evaporation and chemical vapor deposition (CVD). CVD is among the most popular and widely applied techniques due to their convenient operation, can be carried out at a lower temperature, has a lower set-up cost, and has a higher production yield compared to other methods [3]. Camphor ($C_{10}H_{16}O$) is a valuable material in nanotechnology and biotechnology study which employ as a precursor with the significant feature in CNT syntheses [4]. Vertically well-aligned CNTs are highly desirable for FE applications that may be effectively assessed and incorporated into devices.

Recent advances have been made in relation to manufacturing vertically-aligned CNTs on a substrate. Although, the adhesion of CNTs to the substrates and the stability of CNT field-emitters remain to be main issues. Porous silicon (PSi) template is an ideal substrate for growing self-oriented nanotubes on a large area. In this work, PSi nanostructures were applied as a substrate to grow CNTs. Vertically-aligned multilayer CNTs were successfully synthesized using a novel technique which includes improving the catalyst-nanotemplate interaction in the CVD method, indicating a unique tip shape and excellent field electron emission properties.

2. EXPERIMENTAL

Electrochemical anodization method was employed to fabricate the PSi substrate by doped p-type Si (100) with $525 \pm 25 \mu\text{m}$ thick wafers. In this process, a mixture of 48% hydrofluoric acid and 99.7% absolute ethanol was provided at a ratio of 1:1 by volume [5, 6]. Si substrate and Pt wire were used as the anode and cathode respectively. Electrochemical etching was done at a fixed current density of 20 mAcm^{-2} for 20 min. A halogen light bulb was employed to aid the etching process by maintaining and accelerating the etching rate.

Vertically-aligned CNTs deposited on a PSi substrate were synthesized by a two-stage tube furnace system prepared with a single alumina tube. 5.33 wt.% of ferrocene was carefully blended in Camphor oil as a precursor, and 4 ml of the mixture was positioned in an alumina boat located side-by-side in the first furnace to release the vaporized CNTs. Then, PSi substrates were located at the center of the second furnace. Before the synthesis process, the tube was flushed with argon (Ar) gas through the tube end of first furnace for 10 min. Then, the precursor furnace was heated to $180 \text{ }^\circ\text{C}$ for the precursor vaporization process. In a typical deposition process, the temperature of the second furnace was increased to $750 \text{ }^\circ\text{C}$, prior to increasing the temperature of the first furnace to $450 \text{ }^\circ\text{C}$.

Three low rates of Ar gas flow were utilized at 1 bar to generate three separated growth sequences of multilayer CNTs. Ar gas was injected into the inlet tube with a syringe pump at a maximum flow of 200 standard cubic centimeters per minute (sccm) for 20min. Then, the flow rate was gradually increased to 400 sccm. After 20min, the low rate was increased to 600 sccm until

complete consumption of the carbon source. After the multilayer CNTs was synthesized onto the PSi substrate, both furnaces were permitted to cool to room temperature under a continuous Ar gas flow. FE scanning electron microscopy (FESEM; ZEISS 77 Supra 40VP) was used to examine the CNTs growth morphology. In addition, crystallinity of samples was characterized by micro-Raman spectroscopy with a laser of 514 nm (Horiba Jobin Yvon 79DU420A-OE-325).

To analyze FE properties of the samples, the vertically aligned CNTs film was used as the cathode, and a mirror-polished silicon wafer (as the anode substrate) was located parallel over the upper surface of the CNTs film. The gap between the anode and cathode was approximately 500 μm . The FE properties were evaluated under a vacuum of $\sim 10^{-6}$ Torr with the voltage application of 0-2000 V between the two electrodes.

3. RESULTS AND DISCUSSION

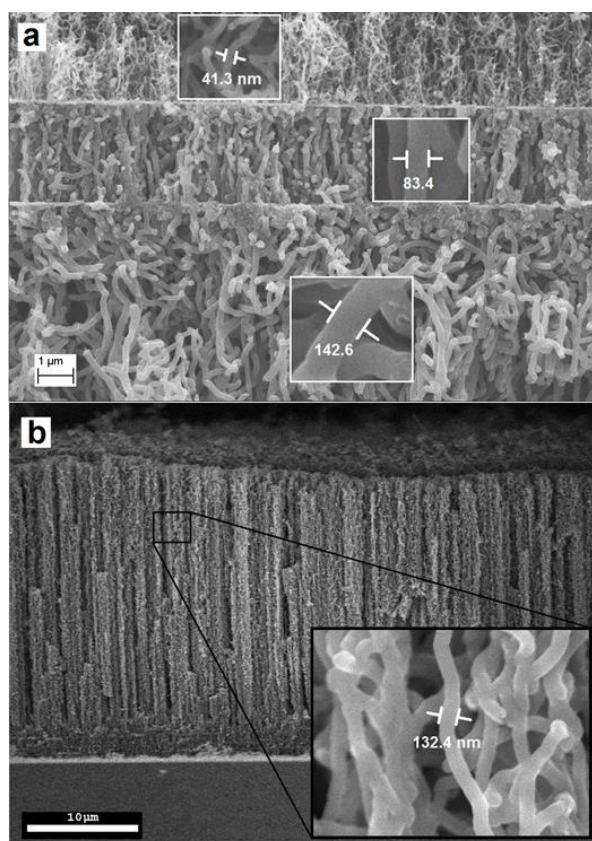


Figure 1. Cross-sectional FESEM images of (a) multilayer and (b) as-deposited VACNTs.

Figure 1 shows the cross-sectional FESEM images of the vertically aligned tribble layer and as-deposited carbon nanotube film produced by using a two-stage tube furnace mechanism. This technique assisted to the growth of multilayer CNTs in the form of large-scale aligned arrays, without the requirement to any additional catalyst. Furthermore, as revealed in Figure 1a, the length and packing density of the aligned nanotubes in every layer can vary by choosing different synthetic routes,

and/or changing the experimental conditions. This means that the CNT length and of each layer is controlled by the growth time and gas flow rate of its respective sequence. Figure 2 indicates that the Raman spectrum of the CNTs film displayed two typical peaks at around 1352 and 1579 cm^{-1} for the D and G peaks respectively. There is a sharp G peak, which indicates a relatively good long range order for the CNTs.

The G peak is significantly shifted from 1575 to 1584 cm^{-1} for the multilayer VACNTs, which indicates that the electronic structure of CNTs is modified with a new configuration. The G-band is related to E_{2g} mode that agrees to the movement of the two neighboring carbon atoms in opposite directions within the crystalline or the ordered graphene sheet.

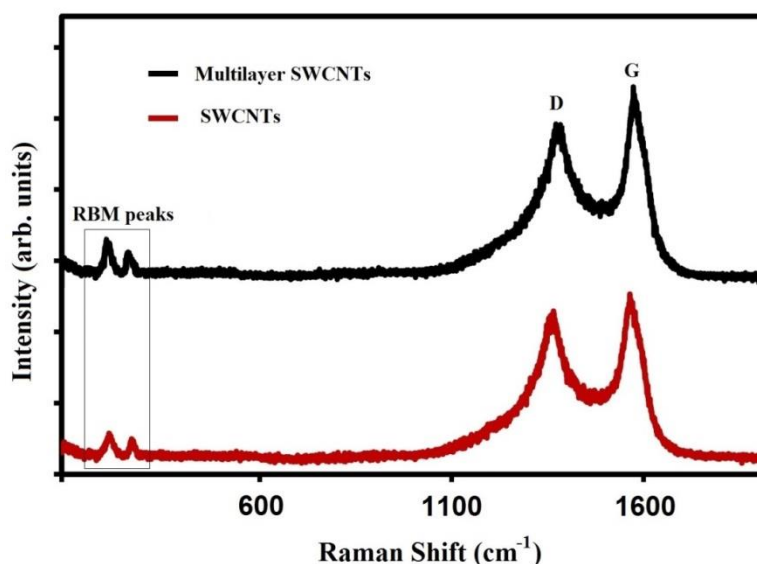


Figure 2. Raman spectrum of multilayer and as-synthesized SWCNTs.

The D-band was attributed to the A_{1g} breathing mode, which is associated with the defects in a graphite sheet, sp^3 carbon clusters, or other impurities. The intensity ratio of the I_D/I_G values is a measure of the defects present on CNTs, and a greater degree of graphitic crystallinity, which acts as an effective emission site. From the Raman spectrum, a smaller value of I_D/I_G (0.867) was observed for the multilayer VACNTs compared to as-synthesized VACNTs.

The radial breathing mode (RBM) peaks appeared to be in the range of 200–400 cm^{-1} which indicate the presence of SWCNTs in the sample (as shown in Figure 2) [7].

The very intensive RBM peaks were in the range of 210–280 cm^{-1} , ascribable to the metallic nanotubes, showing that the as-synthesized SWNT sample includes a large percentage of the metallic nanotubes [8].

The diameter (d) of the SWCNTs can be estimated from the RBM peak position (ω) as $d=248$ ($\text{cm}^{-1}\text{nm})/\omega(\text{cm}^{-1})$. The numerical majority of the SWCNTs are found to have a diameter of about 1.15 nm and 0.9 nm for the peaks at 217 and 277 cm^{-1} respectively.

Figure 3 indicates the current density (J) versus the applied electric field (E) plot of multilayer and as-deposited of vertically aligned SWCNT arrays.

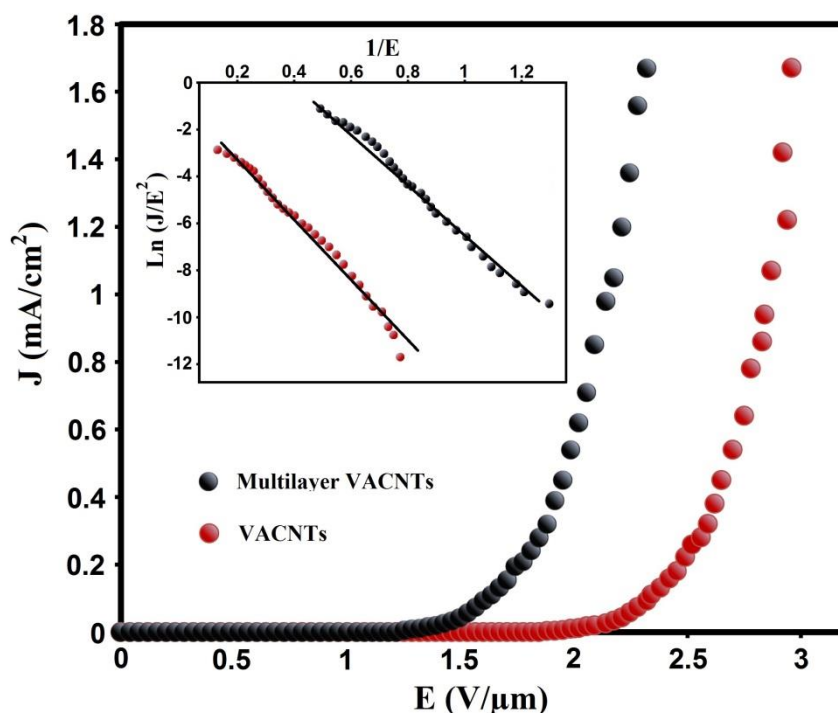


Figure 3. Field emission current density vs applied electric field (J–E) for multilayer and as-synthesized VACNTs. (In inset: The FN plots for the various samples)

The emission characteristics show a Fowler-Nordheim (FN) type behavior [9]. Thus, the relationship between J and E can be expressed by the equation:

$$J = \frac{1.56 \times 10^{-6} \beta^2 E^2}{\varphi} \exp\left(-\frac{6.83 \times 10^3 \varphi^{3/2}}{\beta E}\right) \tag{1}$$

where J is the emitter current density (A/cm²), E is the applied electric field, φ is the work function of the emitter material and β is the field enhancement factor [10].

The turn-on field (E_{to}) and the threshold field (E_{thr}), which are specified as the macroscopic electric field required to produce a current density of 10 nA/cm² and 1 mA/cm² [11], are about 1.31 and 2.16 V/μm for multilayer VACNT structures, and 2.06 and 2.86 V/μm for as-deposited VACNTs, respectively. Both E_{to} and E_{thr} for the multilayer VACNTs are lower than the corresponding values for the as-deposited VACNTs, indicating that the electron FE properties of multilayer VACNTs were significantly enhanced. The better field emissions of synthesized multilayer VACNTs can be attributed to gradually reducing radius of the CNTs and the sharpness of the emission sites.

The FN plots for the various samples are revealed in the inset of Figure 3. The field enhancement factor can be considered from the slope of the FN plot. The inset of Figure 3 shows well conformity and linearity to the FN tunneling emission mechanism for both samples. Based on the slope of the FN plot, β was estimated to be approximately 2896 and 3837 for multilayer and as-deposited VACNTs, respectively, when setting the $CNT = 4.7$ eV work function [12]. The field enhancement factor of the multilayer VACNTs grown on PSi is relatively higher compared to those of the as-deposited VACNTs, which might be attributed to the appropriate constructive morphology and crystal structure.

4. CONCLUSION

Multilayer VACNTs were successfully synthesized on PSi substrate by a two-stage hot filament assisted CVD method using camphor oil as a carbon source. Resonance Raman behavior of the VACNTs films approves the presence of graphitic carbon, based on the presence of the G-band peak at 1593 cm^{-1} , while the RBM peaks between 100 and 400 cm^{-1} confirm the presence of SWCNTs. A weak D-band peak shows high-purity SWCNTs.

It was obviously considered that the FE current density gradually increased for multilayer VACNTs. This observation can be attributed to highly sharp tips and the improvement of the phase purity. The remarkably high current density was attained under a relatively low applied electric field, suggesting that the VACNTs are able to use as efficient electron field emission sources for various applications such as flat panel displays.

ACKNOWLEDGEMENTS

The authors gratefully acknowledge that this work was partially supported by the Department of Physics in Shahid Beheshti University and the Universiti Teknologi Petronas grant number UTP-URIF-0153AA-B96. Furthermore, the authors are grateful to the Institute of Research Management and Innovation (IRMI), Universiti Teknologi MARA (UiTM) and the Deanship of Scientific Research, King Saud University (KSU) for their support through Vice Deanship of Scientific Research Chairs.

References

1. J.-W. Kim, J.-W. Jeong, J.-T. Kang, S. Choi, S. Park, M.-S. Shin, S. Ahn and Y.-H. Song, *Carbon*, 82 (2015) 245-53.
2. Z. Spitalsky, D. Tasis, K. Papagelis and C. Galiotis, *Prog. Polym. Sci.*, 35 (2010) 357-401.
3. N. De Greef, L. Zhang, A. Magrez, L. Forró, J.-P. Locquet, I. Verpoest and J.W. Seo, *Diam. Relat. Mater.*, 51 (2015) 39-48.
4. M. Kumar, T. Okazaki, M. Hiramatsu and Y. Ando, *Carbon*, 45 (2007) 1899-904.
5. N. Naderi, M. Hashim, J. Rouhi and H. Mahmodi, *Mat. Sci. Semicon. Proc.*, 16 (2013) 542-6.
6. N. Naderi, M. Hashim, K. Saron and J. Rouhi, *Semicond. Sci. Technol.*, 28 (2013) 025011.
7. Y. Piao, J.R. Simpson, J.K. Streit, G. Ao, M. Zheng, J.A. Fagan and A.R. Hight Walker, *ACS Nano*, 10 (2016) 5252-9.

8. C. Luo, D. Wan, J. Jia, D. Li, C. Pan and L. Liao, *Nanoscale*, 8 (2016) 13017-24.
9. J. Rouhi, M. Alimanesh, S. Mahmud, R. Dalvand, C.R. Ooi and M. Rusop, *Mater. Lett.*, 125 (2014) 147-50.
10. J. Rouhi, S. Mahmud, S.D. Hutagalung, N. Naderi, S. Kakooei and M.J. Abdullah, *Semicond. Sci. Technol.*, 27 (2012) 065001.
11. S. Chen, M. Shang, Z. Yang, J. Zheng, L. Wang, Q. Liu, F. Gao and W. Yang, *J. Mater. Chem. C*, 4 (2016) 7391-6.
12. Y.-J. Huang, H.-Y. Chang, H.-C. Chang, Y.-T. Shih, W.-J. Su, C.-H. Ciou, Y.-L. Chen, S.-i. Honda, Y.-S. Huang and K.-Y. Lee, *Mat. Sci. Eng. B*, 182 (2014) 14-20.

© 2018 The Authors. Published by ESG (www.electrochemsci.org). This article is an open access article distributed under the terms and conditions of the Creative Commons Attribution license (<http://creativecommons.org/licenses/by/4.0/>).